PRAMANA
— journal of
physics

Vol. 52, No. 6
June 1999
pp. 623–629

Thermal lens measurement technique in end-pumped solid state lasers: Application to diode-pumped microchip lasers

RAKESH KAPOOR, P K MUKHOPADHYAY, JOGY GEORGE and S K SHARMA
Center for Advanced Technology, Indore 452 013, India
Email: rkapoor@cat.ernet.in

MS received 13 November 1998; revised 12 May 1999

Abstract. A simple derivation, which relates the thermal lens focal length in solid state lasers to pump power and a method for direct estimation of thermal lens focal length, is reported. This method is applicable to any type of stable resonator. The method is used for the measurement of the thermal lens focal length with an accuracy of 8% in an axially pumped microchip laser. The variation of focal length with pump power is also measured.

Keywords. Thermal lens; microchip laser; diode pumping.

PACS Nos 42.60; 42.55

1. Introduction

Since the development of efficient high-power laser diodes and new solid state laser materials, the end-pumped solid state lasers have generated considerable interest. In these solid state lasers the absorbed pump power generates a temperature profile across the gain medium. This temperature profile gives rise to variation of refractive index across the gain medium. The lens formed due to this refractive index variation is known as thermal lens and it can be negative or positive depending upon the thermal properties of the material. For efficient operation, the pump power induced thermal lens in the laser material became an important factor for optimization of these lasers. There are several theoretical models and experimental methods reported in the literature [1–11] for the determination of the focal lengths of these thermal lenses. In the case of end-pumped system, due to the small size of the pumping profile it is not possible to scan the thermal lens with a probe laser [5, 6]. Beat frequency method [9] and mode degeneration method [10] require multi-mode operation of the laser and if the thermal lens is astigmatic in nature then these methods become complicated. The divergence measurement method [8] is a simple approach to measure thermal lens but the analysis provided in that work is applicable to only simple two mirror resonators.

In this work, with simple physical arguments we could relate thermal lens focal length with pump power. Our approach not only takes care of the thermal lens but also any modification to it due to any kind of mechanical stress and strains present in the laser

crystal. We are also reporting a method for direct estimation of thermal lens. Our method is somewhat similar to the one reported earlier [8] but our approach is applicable to any type of stable resonator. We have used this method for the measurement of the thermal lens in an axially pumped Nd:YVO_4 microchip laser. We also measured the variation of focal length with pump power.

2. Theoretical analysis

In any solid state laser, the accumulated phase change due to absorbed pump power across the gain medium $\Delta\phi(x,y)$ is

$$\Delta\phi(x,y) = P_{\text{abs}}\Phi(x,y), \tag{1}$$

where P_{abs} is the total absorbed power, as in all circumstances, the phase variation will be proportional to the total power absorbed by the gain medium. $\Phi(x,y)$ is a normalized proportionality function which will mainly depend upon the geometry, thermal properties of the gain medium, and the shape of the pump beam profile. These phase profiles are responsible for thermal lens effects in a laser. The phase change across any thin lens of focal length f is given as follows [12]

$$\Delta\phi_f = \frac{kx^2}{2f}, \tag{2}$$

where k is the wave number. Expanding the function $\Phi(x,y)$ as a polynomial

$$\Phi(x,y) = a_0 + a_{1x}x + a_{1y}y + a_{2x}x^2 + a_{2y}y^2 + a_{2xy}xy + \cdots, \tag{3}$$

a comparison of (3) with the thin lens expression in (2) shows that the quadratic term in $\Phi(x,y)$ will always act as a thin lens in a resonator. In a stable resonator, out of all the components of the accumulated phase profile only the thin lens formed due to quadratic term will affect the Rayleigh range or the radius of the TEM_{00} mode. All other terms except the constant will be responsible for wavefront distortion in each round trip. These distortions will increase the intracavity losses due to scattering or refraction. With the help of (2) and (3), the expression for the focal length of the thermal lens across the x- and y-axis of the gain medium can be given as

$$f_i = \frac{k}{2P_{\text{abs}}\, a_{2i}}, \tag{4}$$

where i stands for x or y. Besides these thermal effects, mechanical stress can also cause variation of the phase profile across the medium, although the mechanical stress due to absorbed pump power are taken care by the thermal lens itself. The mechanical stress due to other factors like mounting of crystals can give rise to the change in refractive index profile across the medium. If f_m is the focal length of the lens generated due to these mechanical factors and s is the separation between the thermal and the mechanical lenses, then the effective focal length f_e will be given as

$$f_{ei} = \frac{1}{(2\,P_{\text{abs}}\, a_{2i}/k)(1-(s/f_m)) + (1/f_m)}. \tag{5}$$

The absorbed pump power in a laser medium is proportional to the incident pump power and the quantities s, f_m, a_{2i}, and k given in (5) are constants, therefore the expression for effective focal length can be rewritten as

$$f_e = \frac{1}{\alpha P_{\text{pump}} + \beta}, \tag{6}$$

where all the constants are reduced to constants α and β. These constants will vary significantly from laser to laser. Therefore on-line measurement of the thermal lens focal length in a laser is always a better proposition. For the measurement of f_e we have used the following approach. Any resonator can be described in terms of an infinite wave-guide of repeated optical components. The reduced complex radius of curvature [12] q at any plane inside the resonator can be obtained from the solution of the following quadratic equation

$$Cq^2 + (D - A)\, q - B = 0, \tag{7}$$

where A, B, C, and D are matrix elements of an $ABCD$ matrix which corresponds to optical path for one round trip starting from the relevant plane inside the resonator. This $ABCD$ matrix is obtained from the individual $ABCD$ matrices of the resonator components. In these optical components, a thin lens of unknown focal length f_e, corresponding to a thermal lens, is included at the gain medium location. In the combined $ABCD$ matrix, values corresponding to all other optical components are known except the thermal lens focal length f_e. Once the reduced complex radius of curvature is known at any plane inside the resonator, it is very easy to locate the position of the beam waist inside the resonator. The reduced complex radius of curvature q_0 at the waist plane, obtained as a function of f_e, is related to waist size ω_0 by

$$\omega_0(f_e) = \sqrt{\frac{-iq_0\,(f_e)\,\lambda}{\pi}}, \tag{8}$$

where λ is the laser wavelength in vacuum, $q_0 = iz_R$ and z_R is the Rayleigh range. If the output coupler does not modify the laser beam, the far-field beam size of the laser output can be measured to calculate the waist size with the help of the following relation

$$\omega(z) = \omega_0 \sqrt{1 + \left(\frac{z\lambda}{\pi\omega_0^2}\right)^2}, \tag{9}$$

where $\omega(z)$ is the far field spot size of laser beam at a distance z from beam waist. With the help of (8) and (9), the value of the thermal lens focal length f_e is obtained from the experimentally measured ω_0 value using a numerical iteration method. With a TEM_{00} output profile the beam size is obtained by fitting a Gaussian curve to the experimentally recorded far field profile. In case the higher order modes are also present, the far field spot size can be easily obtained either by fitting a mixture of Hermite Gaussian profiles of different orders or by estimating the beam quality factor M^2. The multi-mode far-field spot size $W(z)$ at a distance z from the beam waist is given as [13]

$$W(z) = M\omega_0 \sqrt{1 + \left(\frac{z\lambda}{\pi\omega_0^2}\right)^2}. \tag{10}$$

Here we are making use of the fact that in a stable resonator the value of the Rayleigh range z_R is unique for all the modes [13]. In our microchip resonator, the thermal lens makes the resonator stable. The high value of average absorption coefficient ($a = 42\,\mathrm{cm}^{-1}$) keeps the active region confined to the back mirror of the crystal. Therefore we can assume that the thermal lens is located at the back mirror plane. The $ABCD$ matrix M_t for a round trip optical path starting from output window can be given as

$$M_t = \begin{pmatrix} 1-(d/nf) & (2d/n)-(d^2/n^2 f) \\ -(1/f) & 1-(d/nf) \end{pmatrix}, \tag{11}$$

where d is the thickness of gain medium, n is its refractive index and f is the thermal lens focal length to be determined. The value of the Rayleigh range z_R can be obtained with the help of (7) and matrix elements in (11). The waist will be related to these resonator parameters as follows

$$\omega_0^2 = \frac{z_R \lambda}{\pi} = -i\frac{\lambda d}{n\pi}\sqrt{\frac{-2nf}{d}+1}, \tag{12}$$

where values of d, n, λ are known and, for a stable resonator $2f > d/n$.

3. Experimental

The experimental set up for thermal lens focal length measurement is shown in figure 1. An FTI make (Russian) strip type (1 μm × 100 μm) semiconductor diode laser was used as an axial pump source. The diode laser was operated at 809 nm. With a built in fast axis collimator, the far-field divergence angles are $\theta_\perp = 0.9°$ and $\theta_{||} = 8°$. The pump beam was collimated and focused on the gain medium with the help of lenses f_1 and f_2. The gain medium was a 0.5 mm thick, 3 atm% Nd^{3+} doped YVO_4 crystal. The resonator for the microchip laser was formed by directly depositing dielectric mirrors on to the crystal surfaces. The output mirror had a reflectivity of 95.0% at 1064 nm. The opposite mirror had a reflectivity of 99.9% at 1064 nm and transmission of 95.0% at the pump wavelength. This microchip laser shows a slope efficiency of 48.0% with a threshold of 50.7 mW. As the laser output was a mixture of 809.0 nm and 1064.0 nm wavelengths, an edge filter was

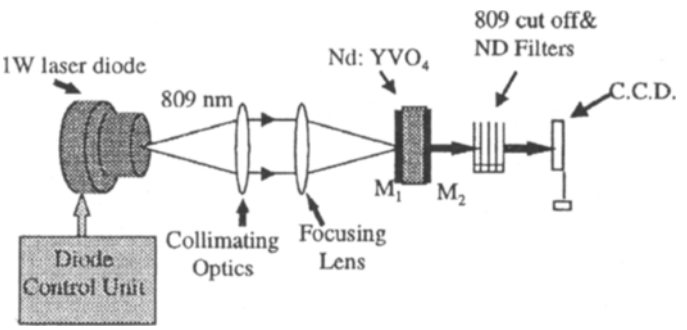

Figure 1. Experimental setup for focal length measurement of thermal lens.

used to block the 809.0 nm emission. Neutral density filters reduced the intensity of the IR laser beam. Intensity profile of the 1064.0 nm laser beam was recorded at a distance of 309.0 mm from the output mirror. The profile recorder was an SBIG CCD camera with a 16-bit dynamic range. The pixel sizes are 23μm and 27μm in the horizontal and vertical directions respectively. The pump power delivered by the diode laser was varied from 180.0 mW to 780.0 mW by changing the diode current. The IR laser profile was recorded at different pump powers. For each profile recording, the thermal lens was allowed to stabilize for 10 min. All recorded profiles were perfectly Gaussian in the vertical direction but started deviating from Gaussian shape in the horizontal direction at higher powers. The beam radius was obtained by fitting a Gaussian profile to both the horizontal and vertical directions. At higher power, the size of the beam was estimated in horizontal direction by fitting a mixture of zeroth and first order Hermite Gaussian intensity profiles. A typical fit to a horizontal profile at 780 mW pump power is shown in figure 2. The size of the beam waist is estimated from these computed far field beam-radius values with the help of (9). The focal lengths of thin lenses in both horizontal and vertical directions were estimated

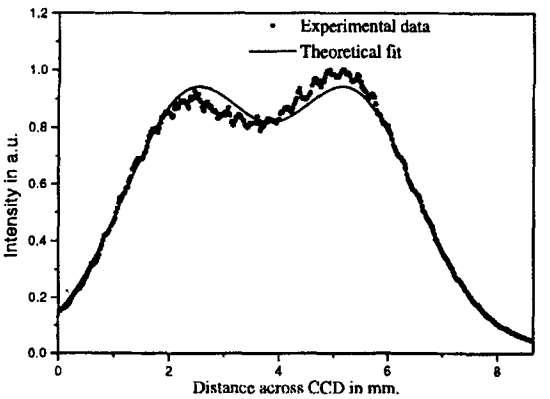

Figure 2. Recorded profile of multimode laser beam at 780 mW pump power. Size of beam was estimated by fitting a mixture of zeroth and first order Hermite Gaussian intensity profiles.

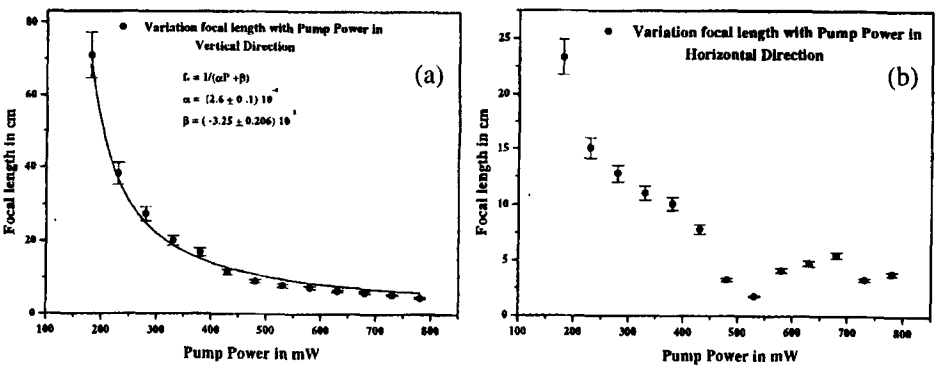

Figure 3. Variation of focal length with pump power (**a**) vertical direction, (**b**) horizontal direction.

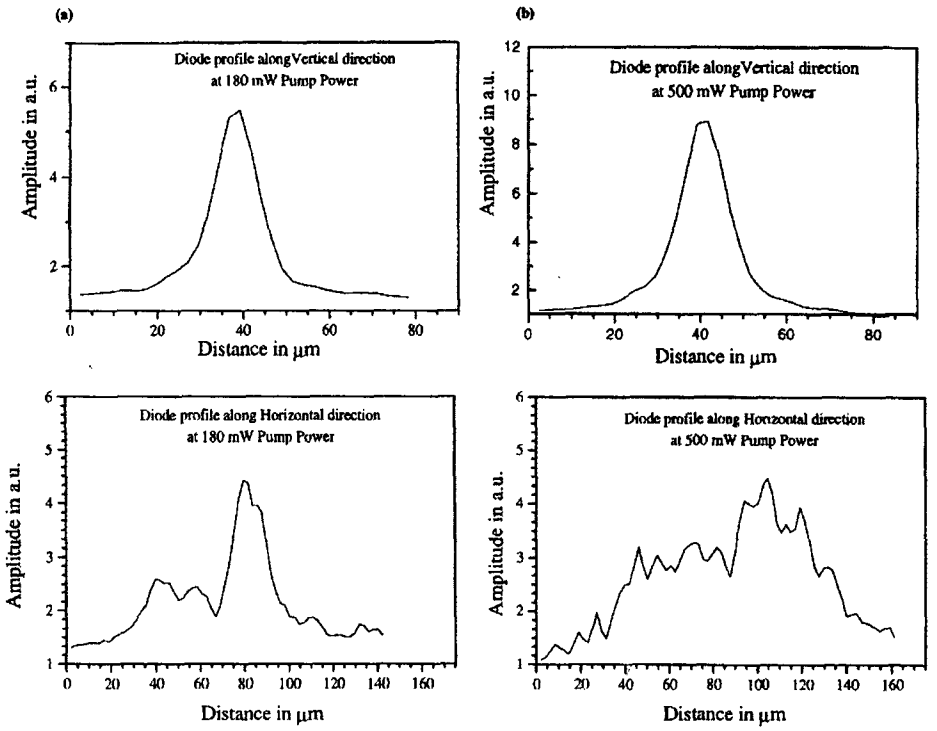

Figure 4. Focused pump beam profiles in the vertical and horizontal directions at 180 mW pump power (**a**), and 500 mW pump power (**b**).

from the computed waist sizes with the help of (12). The measurement error in the thermal focal length was estimated from the maximum possible measurement errors in the far field spot size, crystal thickness and the camera position from the beam waist. The estimated error in the thermal focal length measurement is less than 8%. Figure 3a and 3b show the variation of focal lengths with input pump power in vertical and horizontal directions respectively. The solid line in figure 3a is the theoretical fit to the plot. It shows that thermal lens focal length in the vertical direction varies with pump power as per (6) while, in the case of the horizontal direction, the experimental values are quite different from the theoretical curve. To find out the cause of this deviation from the theoretical value, we recorded the focused profile of the pump beam using the same camera by an imaging technique. The focused pump beam profiles at 180 mW and 500 mW pump powers are shown in figure 4a and 4b respectively. It can be seen that the shape of the pump beam remains the same in the vertical direction but changes in the horizontal direction with power. Therefore, in the horizontal direction the values of α and β in (6) are not constant for different pump powers. This explains the deviation of experimental values from the theoretical fit in figure 3b.

4. Conclusion

We have demonstrated a simple and very accurate method for the on-line measurement of the thermal lens in a solid state laser. We have also shown that the variation of thermal lens

focal length with pump power is as per the relation we have derived. For proper estimation of overlap efficiency and mode volume, the value of thermal lens focal length is required and we have shown that with our method the thermal lens focal length can be obtained directly. While in case of other methods, one only gets the accumulated phase profile and for estimation of thermal lens, the quadratic term has to be extracted from this accumulated phase profile.

Acknowledgements

The authors would like to thank H S Vora for his valuable help in converting SBIG image files to ASCII files.

References

[1] J E Murray, *IEEE J. Quantum Electron.* **QE-19**, 488 (1983)
[2] J M Eggleston, T J Kane, K Kuhn, J Unternahrer and R L Byer, *IEEE J. Quantum Electron.* **QE-20**, 289 (1984)
[3] Herman Vanderzeele, *Opt. Lett.* **13**, 369 (1988)
[4] M E Innocenzi, H T Jura, C L Fincher and R A Fields, *Appl. Phys. Lett.* **56**, 1831 (1990)
[5] D S Sumida, D A Rockwell and M S Mangir, *IEEE J. Quantum Electron.* **QE-24**, 985–994 (1988)
[6] Jason M Eichenholz and Martin Richardson, *IEEE J. Quantum Electron.* **QE-34**, 910–919 (1998)
[7] W Koechner, *Solid-State Laser Engineering*, 3rd ed. (Springer Verlag, Berlin, 1992)
[8] Beat Neuenschwander, Rudolf Weber and Heinz P Weber, *IEEE J. Quantum Electron.* **QE-31**, 1082 (1995)
[9] B Ozygus and J Erhard, *Appl. Phys. Lett.* **67**, 1361 (1995)
[10] B Ozygus and Qincheng Zhang, *Appl. Phys. Lett.* **71**, 2590 (1997)
[11] Justin L Blows, Judith M Dawes and Takashinge Omatsu, *Appl. Phys.* **83**, 2901 (1998)
[12] A E Siegman, *Lasers* (University Science Book, Mill Valley, CA, 1986)
[13] Anthony E Siegman and Steven W Townsend, *IEEE J. Quantum Electron.* **QE-29**, 1212 (1993)